IL NUOVO CIMENTO **47 C** (2024) 345
DOI 10.1393/ncc/i2024-24345-y

COLLOQUIA: MAYORANA 2023

Dark matter direct detection with liquid xenon experiments: Present and future

E. APRILE

Physics Department, Columbia University - New York, NY 10027, USA

received 6 August 2024

Summary. — Experiments using liquid xenon provide the strongest limits on dark matter-nucleon interactions in the weak mass range, and have been able to rapidly scale-up the target mass by several orders of magnitude while reducing backgrounds to ultra-low levels.

1. – Introduction

The majority of the matter in the Universe is made up of dark matter (DM), a non-luminous, rarely interacting form of matter. From measurements of orbital velocities of galaxies in clusters and of individual galactic rotation curves to measurements of the mass of an entire galaxy cluster via gravitational lensing and the distribution of the X-ray emitting gas, from precise measurements of the cosmic microwave background temperature fluctuations and of the abundance of light elements, to the mapping of structures on the largest observed scale, we have a solid evidence for the presence of dark matter. Furthermore, these observations also give us the picture of a Universe which is spatially flat, accelerating, and composed of $\sim$5 % baryonic matter, $\sim$27 % DM and $\sim$68 % dark energy [1]. To-date dark matter has been observed only indirectly, through its gravitational influence on luminous matter. Despite the progress made over the last decades in understanding its distribution on many scales, we still cannot answer the most basic question: what is the fundamental nature of dark matter? Among the many hypothetical dark matter particle candidates which have been proposed over the years, with an assortment of couplings, masses, and detection signatures, the class of Weakly Interacting Massive Particles (WIMPs) has been the most studied both theoretically and experimentally. WIMPs emerge naturally in various extensions of the Standard Model of particle physics but we note that other DM candidates, equally well-motivated theoretically, include axions, or more generally, axion-like particles (ALPs), dark photons and sterile neutrinos [2]. So far all these dark matter particle candidates have eluded direct detection, making the determination of the particle nature of dark matter one of the most urgent and fundamental open problem in cosmology, astrophysics and particle physics.

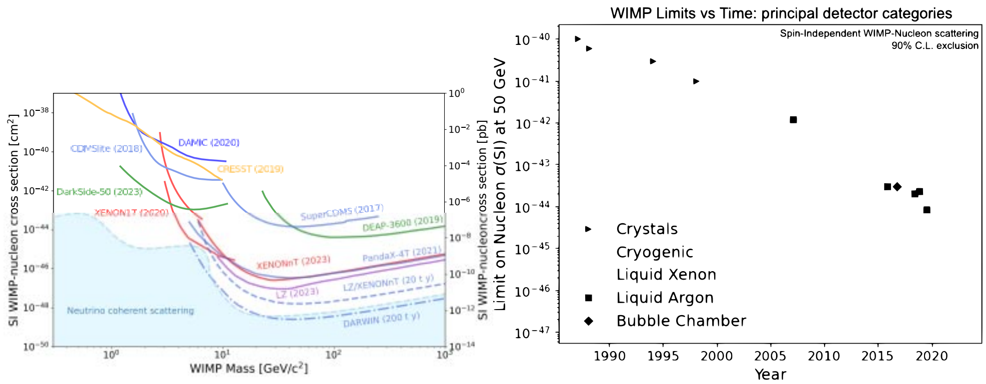

(a) (b)

Fig. 1. – (a) Experimental constraints (solid) and projections (dashed lines) on the spin-independent WIMP-nucleon cross section. Future detectors such as DARWIN aim to cover the experimentally accessible space until the neutrino background will start dominating the rates, illustrated by the neutrino fog [4] (light blue). (b) Upper limit on spin-independent WIMP-nucleon cross section at 50 GeV/c^2 *vs.* time.

In the field of WIMPs direct detection, a wide range of sensitive experiments are being operated in underground laboratories around the world [3] to directly detect WIMPs with a variety of target materials and detector technologies (see fig. 1).

The sensitivity for WIMP masses above $\sim$5 GeV/c^2 is led by experiments using liquid xenon (LZ [5], PandaX-4T [6], XENONnT [7]) and liquid argon (Darkside-50 [8], DEAP-3600 [9]). The low mass region is explored with experiments using crystals operated at mK temperatures (CRESST [10], EDELWEISS [11], SuperCDMS [12]), Si CCDs (DAMIC [13], SENSEI [14]) and low-threshold high-purity Ge diodes (CDEX [15]), and new ideas are being pursued to detect sub-GeV DM candidates [16].

2. – Liquid xenon dark matter experiments

As shown in fig. 1(b), liquid xenon time projection chambers (LXeTPCs) have delivered the best constraints on WIMP-nucleon scattering cross-section for about two decades.and are expected to continue this legacy of excellence for the rest of the decade. See [17] for a recent review of large TPCs for DM and other rare event searches. In a dual phase XeTPC, particle interactions are observed via two distinct signals, as illustrated in fig. 2. The first to be detected, shown to the left, is the prompt scintillation light (S1), while the second is caused by ionization electrons that are drifted and extracted into the gas above the liquid, where they produce electroluminescence (S2). The photons are typically detected by two arrays of photomultiplier tubes (PMTs), and the difference in arrival time between the S1 and S2 signals yields the depth z of an interaction. The S2 light distribution in the top array yields the (x, y)-position of an event, while the S2/S1 ratio allows discriminating electronic recoils (ERs) from nuclear recoils (NRs) [18].

The Xe high atomic mass number and high liquid density allow for massive yet compact, homogeneous detectors with efficient self-shielding against external radiation. The simultaneous detection of both ionization and scintillation signals down to a few keV enables (dual-phase XeTPCs to reconstruct event positions in 3D, in turn allowing for powerful background suppression via fiducialization of the active liquid target.

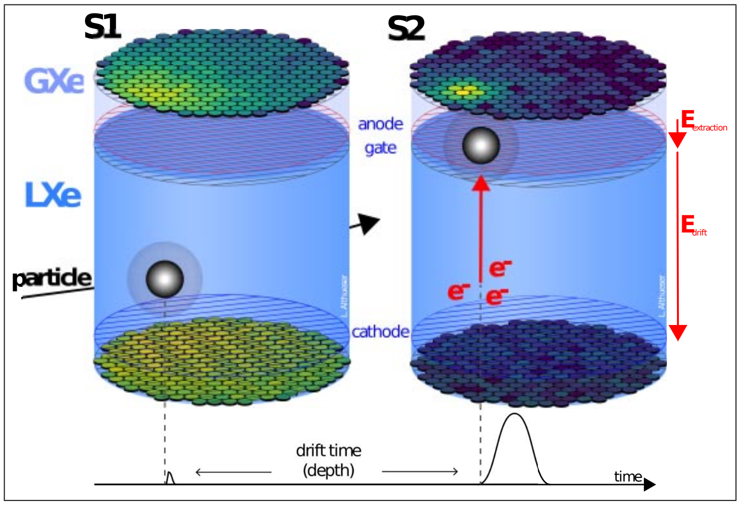

Fig. 2. – Principle of operation of a dual phase XeTPC. In the left figure, an incoming particle deposits energy, and the prompt scintillation light is observed with the top and bottom PMT arrays. On the right, ionization electrons, under the influence of appropriate electric fields, drift to the liquid-gas interface where they are extracted and accelerated producing the S2 signal, observed by the same PMTs.

These features have been exploited and demonstrated by the detectors of the XENON Dark Matter phased program (see fig. 3) carried out since 2005 at the INFN Laboratori Nazionali del Gran Sasso (LNGS) [19], first with the pathfinder XENON10 (14 kg LXe TPC) followed by XENON100 (62 kg LXe), then XENON1T (2.0 t LXe) and the currently operating XENONnT (5.9 t LXe) detector. Results on the WIMP-nucleon scattering cross section achieved by these successive experiments are shown in fig. 4. The unprecedented improvement in sensitivity, with a factor of 10 every ∼3.3 years since ∼2007, was only possible thanks to the drastic concomitant reduction in background levels, with current lowest electronic background rate in XENONnT of ∼.3 events/(t d) in the energy region relevant for WIMPs, below 10 keV. The comparable rate for XENON10 was ∼ 10000 events/(t d).

3. – Current: PandaX-4T, XENONnT and LZ

The current generation of LXe experiments are at the multi-ton scale: PandaX-4T at the China Jinping Laboratory with 5.6 t of LXe (3.7 ˆactive), XENONnT with 8.6 ˆof LXe (5.9 ˆactive)at LNGS, and LZ with 10ˆof LXe (7 ˆactive) at the SURF laboratory. The TPC design for these experiments is rather similar, with a cylindrical structure made of PTFE enclosing the active target viewed by a top and a bottom array of low-radioactivity PMTs. More details of the XENONnT TPC and its current status are given below.

The XENONnT active LXe target is contained in a cylindrical PTFE structure with a diameter of 1.33 m and a height of 1.49 m. A total of 494 Hamamatsu R11410-21 3-inch PMTs [26, 27] distributed in a top and a bottom array view the sensitive volume. A double-walled, low-radioactivity stainless steel cryostat is filled with 8.6 t of LXe and houses the detector. The cryostat is placed in a 700 t water Cherenkov muon veto, 10.2 m high and 9.6 m in diameter, equipped with 84 8-inch PMTs [28]. A volume of 33 m^3

XENON10	XENON100	XENON1T	XENONnT
2005-2007	2008-2016	2012-2019	2020-2026 (taking science data)
14 kg Xe target	62 kg Xe target	2 t Xe target	~6 t Xe target, 8.6t total
~10^{-43} cm^2	~10^{-45} cm^2	4 ×10^{-47} cm^2	Projection: 1.4×10^{-48} cm^2 for 20 tonne-year
~2000000 background ER events/(keV t y)	1800 background ER events/(keV t y)	82 background ER events/(keV t y)	16.1 background ER events/(keV t y)

Fig. 3. – The XENON Dark Matter Experiments at LNGS

of water surrounding the cryostat and delimited by reflectors made of high-reflectivity expanded PTFE is used as a neutron veto, seen by 120 8-inch PMTs. The ultra-pure water is doped with Gd to increase the neutron veto efficiency. A high-throughput radon distillation column was continuously operated to remove radon [29], from the gaseous xenon in the TPC, while a krypton distillation column reduced the ^{nat}Kr concentration

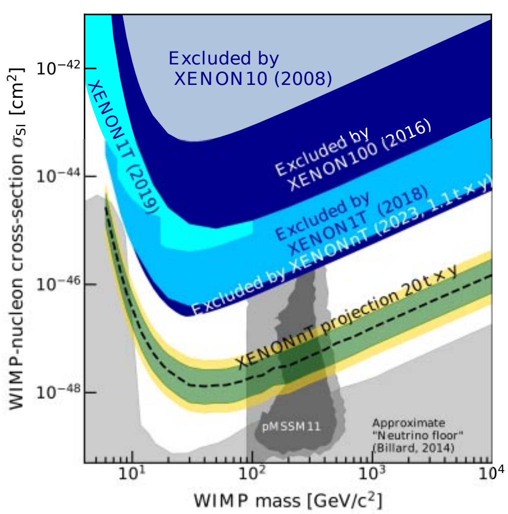

Fig. 4. – The plot shows successive results from the XENON collaboration [7, 20-23]. The gray region at low cross-sections is one estimate of where the astrophysical neutrino flux will dominate over a dark matter signal, from [24], and the contour shows a supersymmetric parameter scan favored region for WIMP dark matter [25].

to < 50 ppq. A novel LXe purification system [30] allowed reaching a very high removal rate of electronegative impurities on a short time scale, with an electron drift lifetime above 15 ms. The dominant electronic recoil background in the first science run was due to β-decays of the ^{222}Rn daughter ^{214}Pb, with a ^{222}Rn concentration of 1.8 μBq/kg. The first science run of XENONnT (SR0) was dedicated to probe the nature of an intriguing excess observed in XENON1T: a peak in the spectrum of electronic recoil events compatible with a 2.3 keV peak from solar axions or from a new background, such a a very small contamination of tritiated hydrogen molecules [31]. The analysis blinding strategy was adapted to also cover signals in the electronic recoil band, and dedicated side-band runs were collected where a tritium signal, if any, would be amplified by bypassing purification systems. The blinding strategy for this first science run was modified to include ER signals as well as NR signals below 20 keV to allow for an unbiased search for both signatures, with a stepwise unblinding of first the ER data and then the NR band. The resulting analysis of 1.16 t y featured the lowest ever background rate achieved in a dark matter detector, 16.1 ± 1.3events/(tonne $\times$ year $\times$ keV), and found no excess. This conclusively ruled out any new physics explanation of the XENON1T excess, and placed strong limits on new physics yielding ER signals. XENONnT also performed a search for WIMPs with the same dataset. The data had no significant excess with respect to the background model ($p > 0.2$) with the lowest upper limit on spin-independent (SI) WIMP-nucleon cross sections of 2.58×10^{-47} cm^2 at 28 GeV/c^2 (90% CL) [7]. XENONnT continues to take data, with a further reduced ^{222}Rn concentration in LXe of 0.8 μBq/kg, using the radon distillation system with combined gaseous and liquid xenon flow. The goal is to continue to explore the sensitivity to WIMPs with a ~ 20 tonne-year exposure as originally planned, as shown in fig. 4. Similar sensitivity is expected from the LZ experiment [32], as shown in fig. 1(b).

4. – Future: DARWIN/XLZD

The success of the XENON program over the years has encouraged and paved the way for the DARWIN concept, a next-generation liquid xenon based experiment with a TPC enclosing a more massive active Xe target (40 t, 50 t total LXe mass) while maintaining a low ($\sim$ 1 keV) energy threshold [33]. The baseline design follows that of the current LXeTPCs. The cylindrical TPC of 2.6 m diameter and height is placed in a low-background titanium cryostat, surrounded by active neutron and muon vetos.

Recently, the XENON, LZ, and DARWIN collaborations joined forces to form the XLZD consortium [34], with the goal of constructing and operating the next-generation experiment together. The size and scope of the detector might be enlarged, compared to DARWIN, with a 3 m$\times$3 m TPC containing 60-80 t of LXe (75-100 t in total). The larger mass would allow for a 3-σ WIMP discovery at a SI cross section of 3×10^{-49} cm^2 at 40 GeV/c^2 mass, and would increase the sensitivity to the neutrinoless double-beta decay of ^{136}Xe. The science potential of a large, dual-phase xenon detector is detailed in [35].

The sensitivity goals of DARWIN/XLZD require that ER and NR rates are below the ones from irreducible astrophysical neutrino interactions, such as those from solar pp and ^{7}Be neutrinos [36]. For ^{222}Rn, which is a background source through its beta-emitting daughter ^{214}Pb, this requires a reduction of one order of magnitude from the 0.8 μBq/kg achieved in XENONnT, see fig. 5, right. This radon suppression is probably the most crucial challenge for a next-generation experiment.

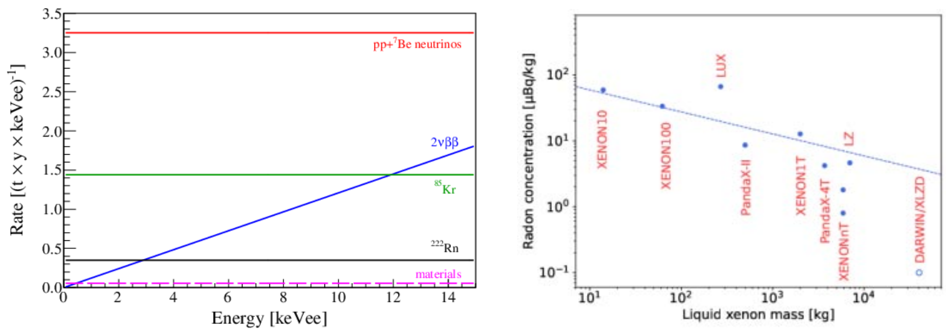

Fig. 5. – (Left) Differential energy spectra of ER background sources in DARWIN. The dominating contribution is from pp- and ^{7}Be solar neutrinos. Figure from [36]. (Right) The evolution of the ^{222}Rn concentration in dual-phase Xe-TPCs (measured values, blue dots), together with the expected decrease from the surface-to-volume ratio (dashed line, $x^{-1/3}$). The goal for DARWIN/XLZD (open circle) is also shown.

Concentrations of < 50 ppq for^{nat}Kr were already achieved by cryogenic distillation [37], which is better than the required ~ 0.1 ppt.

The next-level scale-up to a TPC with 40-60 t target mass poses multiple new technological challenges. A partial list includes: a) mechanical stability of a massive TPC built with only low-radioactivity materials and expected to operate at cryogenic temperature for long periods of time; b) robust and reliable electrodes for establishing the drift/extraction electric fields required for good ER *vs.* NR signals discrimination;c) efficient cryogenic and purification systems capable to handle the massive amount of Xe for a stable and continuous operation over multiple years, and with the highest safety even in case of complete loss of power. Several of these challenges are being studied at various institutions to advance the design of such a larger detector in this decade.

REFERENCES

[1] Aghanim N. *et al.*, *Astron. Astrophys.*, **641** (2020) A6; **652** (2021) C4(E).
[2] Workman R. L. *et al.*, *Prog. Theor. Exp. Phys*, **2022** (2022) 083C01.
[3] Billard J. *et al.*, *Rep. Prog. Phys.*, **85** (2022) 056201.
[4] O'Hare C. A. J., *Phys. Rev. Lett.*, **127** (2021) 251802.
[5] Aalbers J. *et al.*, *Phys. Rev. Lett.*, **131** (2023) 041002.
[6] Meng Y. *et al.*, *Phys. Rev. Lett.*, **127** (2021) 261802.
[7] Aprile E. *et al.*, *Phys. Rev. Lett.*, **131** (2023) 041003.
[8] Agnes P. *et al.*, *Phys. Rev. Lett.*, **121** (2018) 081307.
[9] Lai M., *JINST*, **18** (2023) C02046.
[10] Angloher G. *et al.*, *Eur. Phys. J. C*, **82** (2022) 207.
[11] Armengaud E. *et al.*, *Phys. Rev. D*, **106** (2022) 062004.
[12] Amaral D. W. *et al.*, *Phys. Rev. D*, **102** (2020) 091101.
[13] Aguilar-Arevalo A. *et al.*, *Phys. Rev. Lett.*, **125** (2020) 241803.
[14] Barak L. *et al.*, *Phys. Rev. Lett.*, **125** (2020) 171802.
[15] Xu R. *et al.*, *Phys. Rev. D*, **106** (2022) 052008.
[16] Essig R., Giovanetti G. K., Kurinsky N., McKinsey D., Ramanathan K., Stifter K. and Yu T.-T.,, *Snowmass2021 Cosmic Frontier: The landscape of low-threshold dark matter direct detection in the next decade*, presented at *2022 Snowmass Summer Study* 2022.

[17] Baudis L., *Philos. Trans. R. Soc. London A*, **382** (2023) 20230083, arXiv:2311.05320 [physics.ins-det].
[18] Aprile E., Dahl C. E., DeViveiros L., Gaitskell R., Giboni K. L., Kwong J., Majewski P., Ni K., Shutt T. and Yamashita M., *Phys. Rev. Lett.*, **97** (2006) 081302.
[19] LNGS, `https://www.lngs.infn.it/`.
[20] Angle J. *et al.*, *Phys. Rev. Lett.*, **100** (2008) 021303.
[21] Aprile E. *et al.*, *Phys. Rev. D*, **94** (2016) 122001.
[22] Aprile E. *et al.*, *Phys. Rev. Lett.*, **121** (2018) 111302.
[23] Aprile E. *et al.*, *Phys. Rev. Lett.*, **123** (2019) 251801.
[24] Billard J., Strigari L. and Figueroa-Feliciano E., *Phys. Rev. D*, **89** (2014) 023524.
[25] Bagnaschi E. *et al.*, *Eur. Phys. J. C*, **78** (2018) 256.
[26] Baudis L., Behrens A., Ferella A., Kish A., Marrodan Undagoitia T., Mayani D. and Schumann M., *JINST*, **8** (2013) P04026.
[27] Barrow P. *et al.*, *JINST*, **12** (2017) P01024.
[28] Aprile E. *et al.*, *JINST*, **2014** (P11006) 2014.
[29] Murra M., Schulte D., Huhmann C. and Weinheimer C.,, *Eur. Phys. J. C*, **82** (2022) 1104.
[30] Plante G., Aprile E., Howlett J. and Zhang Y., *Eur. Phys. J. C*, **82** (2022) 860.
[31] Aprile E. *et al.*, *Phys. Rev. D*, **102** (2020) 072004.
[32] Akerib D. S. *et al.*, *Nucl. Instrum. Methods A*, **953** (2020) 163047.
[33] Aalbers J. *et al.*, *J. Cosmol. Astropart. Phys.*, **1611** (2016) 017.
[34] XLZD consortium,, *Website of the XLZD Dark Matter Detection Consortium*, `https://xlzd.org`.
[35] Aalbers J. *et al.*, *J. Phys. G*, **50** (2023) 013001.
[36] Schumann M. *et al.*, *J. Cosmol. Astropart. Phys.*, **1510** (2015) 016.
[37] Aprile E. *et al.*, *Prog. Theor. Exp. Phys*, **2022** (2022) 053H01.